Innovative Infrastructure Solutions (2022) 7:1
https://doi.org/10.1007/s41062-021-00601-1

TECHNICAL PAPER

Using metakaolin-based geopolymer concrete in concrete pavement slabs

M. S. Eisa[1] · **E. A. Fahmy**[2] · **M. E. Basiouny**[1]

Received: 8 May 2021 / Accepted: 25 July 2021 / Published online: 12 October 2021

Abstract
Geopolymer concrete is a new kind of environmentally friendly concrete. It gains early strength in room temperature without water curing, and by heating, strength continues to develop. This study investigates the possibility of using geopolymer concrete based on metakaolin (GPC) as a rigid pavement concrete slab material and as an efficient alternative to conventional Portland cement concrete (PCC). Different constitutes materials of GPC and PCC were tested to assure validity for use. Both GPC and PCC mixtures had 30 MPa compressive strength. GPC specimens were cured at room temperature, whereas PCC specimens were cured in water. GPC mixture was mixed at 2.5 alkaline solutions ratio, and the concentration of NaOH solution was 16 molar. The ratio of SiO_2 to Na_2O in Na_2SiO_3 solution was two. Compressive, flexural, and indirect tensile strength tests, as well as static modulus of elasticity, Poisson's ratio tests and resistance to fuel tests, were performed on both GPC and PCC specimens. To study the behavior of rigid pavement slabs, 800 × 800 × 50 mm GPC and PCC slabs were subjected to mechanical loading tests in three positions (interior, edge and corner). The slabs were supported by a set of steel springs under a 20-mm layer of recycled rubber which had the same surface dimensions of the tested slabs to simulate a subgrade with a modulus of reaction of 36 MPa/m. GPC exhibited a comparable performance with PCC in all investigated parameters in this study with higher rigidity and resistance to surface abrasion in fuel resistance test.

Keywords Rigid pavement slab · Metakaolin · Geopolymer concrete · Ordinary Portland cement concrete (PCC)

Introduction

Concrete pavement is mainly used in weak-soil locations and all places exposed to petroleum leakage such as fuel stations, airport aprons, land ports and garages due to its resistance to fuel attack as opposed to flexible pavement. Geopolymer concrete (GPC) is an efficient alternative to Portland cement concrete (PCC) as a rigid pavement concrete slabs' material due to the following: Metakaolin-based GPC has a satisfactory performance in terms of thermal volumetric changes [1]. GPC can be cured in ambient temperature, in addition to its early strength gain [2, 3]. Previous research works have proved that strength continues to increase by heating [4]. GPC resists acid and sulfate attack due to the non-formation of ettringite in GPC (unlike any other cement hydration components) [5–7]. In addition to the previous advantages of GPC, GPC is an eco-friendly concrete as it is produced without using any Portland cement, as during the production of Portland cement large amount of carbon dioxide is emitted and huge amount of energy is consumed [8, 9]. The geopolymer binder could be formed by three-dimensional polymer chain called geo-polymerization reaction. Geo-polymerization reaction is a chemical reaction between aluminosilicate source such as metakaolin (or any materials that are rich in aluminum and silicon oxides) and alkaline solutions or activator solutions such as NaOH and Na_2SiO_3 [10]. Sinai quarries are the main sources of kaolin in Egypt with annual production of 100 thousand tonnes [11] and as informed by quarries' official website [12]. Kalabsha quarry in Aswan is also a kaolin source in Egypt with

✉ E. A. Fahmy
elsayed.fahmy@hbrc.edu.eg

M. S. Eisa
mohamedeisa524@bhit.bu.edu.eg

M. E. Basiouny
mohamed.bassyoni@bhit.bu.edu.eg

[1] Department of Civil Engineering, Benha Faculty of Engineering, Benha University, Benha, Egypt

[2] Building Materials Research and Quality Control Institute, Housing and Building National Research Center, P.O. 11511, Giza, Egypt

annual production of 60 thousand tonnes [13]. The Egyptian kaolin could be transformed to metakaolin by heating at 800 °C [11]. Many researchers investigated the mix design of GPC [14–19] and drying shrinkage of GPC [1, 20]. GPC demonstrated an adequate performance in terms of drying shrinkage and thermal expansion [1, 21]. The micro-filler effect, nuclear effect, and/or pozzolanic reaction of the MK resulted in less and slower evaporation of water in the MK blended cement paste with low porosity and refined pore's structure when compared with plain concrete, resulting in reduced drying shrinkage [22]. In an investigation of partially replacing cement with metakaolin cement concrete, it was found that replacing cement with metakaolin up to 20% demonstrated remarkable lower shrinkage in comparison with plain concrete. This partial replacement of metakaolin provided an acceptable improvement in the pore structure of concrete and decreased the total porosity up to 49% [23].

The above advantages make GPC an acceptable choice as a concrete slab material in rigid pavement systems. Therefore, the aim of this study was to investigate the possibility of using metakaolin-based geopolymer concrete in rigid pavement concrete slabs by testing the physical and mechanical properties of metakaolin-based GPC and compare it with traditional PCC through evaluating their performance in compression, flexure and splitting tensile in addition to determining their modulus of elasticity, Poisson's ratio and evaluate their resistance to surface abrasion in the presence of fuel attack. The behavior of PCC and GPC slabs was studied by recording loads and vertical deflections under traffic axle loads at interior, edge and corner locations that is known as Westergaard's load cases [24]. Westergaard's load cases were the key for all thickness—design methods for rigid pavement such as Portland Cement Association (PCA) [25] and American Association of State Highway and Transportation Officials (AASHTO) [26] and design manuals such as Yoder EJ [27] and Rigid Pavement Design Manual of Florida Department of Transportation. [28]. PCA and AASHTO methods are dependent on experimental outputs and materials' mechanical properties. To study the behavior of metakaolin GPC slabs under Westergaard's load cases, an experimental model of rigid pavement section was built with concrete slabs of dimensions (800 × 800 × 50) mm to test both GPC and PCC slabs. Steel springs and a 2-cm concrete layer were used to simulate subgrade soil of modulus of reaction ($k = 36$ MPa/m) under the tested slabs as performed in the previous researches [42, 43]. These studies [42, 43] investigated the flexural performance of rigid pavement slabs that reinforced with geogrids experimentally by using Westergaard's load cases and selected one slab for one load case. In this study, three PCC slabs and three GPC slabs were prepared to simulate each load case as one GPC slab was tested for one load case and compared with the oppose PCC slab.

Materials

Metakaolin

Kaolin is a soft, lightweight, often chalk-like sedimentary rock that has an earthy odor. It is white, grayish-white, or slightly colored. Kaolinite is formed mainly by decomposition of feldspars (potassium feldspars), granite, and aluminum silicates. The process of kaolin formation is called kaolinization. Kaolinite is a hydrous aluminum silicate, and it is a crystalline material. Geopolymerization reaction needs an aluminosilicate amorphous material. Consequently, the crystalline kaolinite is calcined to transform into an amorphous aluminosilicate material that is metakaolin [29]. Metakaolin is obtained by calcining the Egyptian kaolinite at 800 °C for 2 h [9]. Metakaolin chemical composition before and after calcination and ASTM C618 [30] requirements are shown in Table 1.

Cement

The used cement was CEM I 42.5 N. Physical and mechanical properties of the used cement are shown in Table 2. The results satisfied EN 197–1 requirements [31] and Egyptian standards specifications [32].

Table 1 Chemical composition and physical properties of kaolin and metakaolin

Elements	SiO_2	Al_2O_3	Fe_2O_3	CaO	MgO	SO_3	K_2O	TiO_2	CL^-	Loss on ignition	Sp.Gr	Sp.Surface area
Kaolin %	52.22 Σ = 84.32%	30.12	1.98	0.10	0.10	0.01	0.07	2.10	0.05	13.25	2.68	2185 (m^2/kg)
Metakaolin %	57.81 Σ = 94.5%	34.97	1.72	1.05	0.54	0.03	1.17	0.79	0.04	1.88	2.57	3950 (m^2/kg)
Requirements*	($SiO_2 + Al_2O_3 + Fe_2O_3$) Min. 70%			–	–	Max. 3%	–	–	–	Max. 6%	–	–

*As per ASTM C618 for Class F pozzolan

Table 2 Cement physical and mechanical properties

Property	Standards	Results	*Specifications [33, 34]
Soundness (Le-Chatelier method) (mm)	EN 196-3	1.0	≤ 10
Initial setting time (min.)	EN 196-3	170	≥ 60
Final setting time (min.)	EN 196-3	205	–
Specific surface area (m^2/kg)	EN 196-6	450	–
Specific gravity	EN 196-6	3.15	–
Flexure strength @ 2 days (MPa)	EN 196-1	4.8	–
Flexure strength @ 28 days (MPa)	EN 196-1	9.8	–
Compressive strength @ 2 days (MPa)	EN 196-1	15.5	≥ 10
Compressive strength @ 28 days (MPa)	EN 196-1	47.8	42.5 ≤ X ≤ 62.5

* EN 197-1 [33] and E.S.S. 4756-1 [34] specifications

Table 3 Properties of aggregates

Property	Standards	Crushed stone aggregates	Fine aggregates	*ECP specifications [35]
Bulk density (g/cm^3)	EN 1097-6	1.58	1.45	–
Fine particles percent (%)	EN 933-1	0.88	1.20	≤ 2.5%
Water absorption (%)	EN 1097-6	1.12	1.20	≤ 2.5%
Fineness modulus	EN 12,620	–	3.09	–
LA abrasion (%)	EN 1097-2	25	–	≤ 30%
Shape index (%)	EN 933-4	12.1	–	≤ 25%
Flakiness index (%)	EN 933-3	18.0	–	≤ 25%

*ECP 203–2018 for concrete structures [35]

Aggregates

Coarse aggregates used in PCC and GPC mixtures were locally crushed stones from Attaka quarry, Suez Governorate, Egypt. Coarse aggregates size ranged from 20 to 10 mm. Fine aggregates used were sand from Abu agwa quarry, Giza Governorate, Egypt. Table 3 shows the physical and mechanical characteristics of both coarse and fine aggregates. Egyptian Code of Practice requirements [33] are listed too. Table 4 shows fine and coarse aggregates sieve analyses.

Activator solution (Alkaline solution)

Sodium hydroxide solution (NaOH)

Sodium hydroxide (NaOH) solutions formed the first half of the alkaline solution used in preparing GPC mixtures. NaOH solution had a concentration of 16 molar. NaOH solution was left to cool down to room temperature for 24 h from its preparation due to its high exothermal temperature that is generated during dissolution.

Sodium silicate solution (Na_2SiO_3)

Table 4 Fine and coarse aggregates sieve analysis

Sieve (mm)	Cumulative percentage passing (%)		
	Fine aggregate	Coarse aggregate (size 10 mm)	Coarse aggregate (size 20 mm)
32.0	100.00	100.00	100.00
22.4	100.00	100.00	98.82
16.0	100.00	100.00	39.94
11.2	100.00	95.60	2.91
8.0	100.00	48.59	0.36
5.6	100.00	10.92	–
4.0	97.06	0.40	–
2.0	91.39	–	–
1.0	66.97	–	–
0.5	33.23	–	–
0.25	2.84	–	–
0.125	0.00	–	–
0.063	0.00	–	–

*As per EN 933-1

Sodium silicate (Na_2SiO_3) solution formed the second half of the alkaline solution used in preparing GPC mixtures. Na_2SiO_3 solution was at liquid gel state. It is locally available with total solids of 44.1% and water of 55.9% by mass.

Water

Portable water was used in this study as mixing water and for diluting NaOH flakes to prepare NaOH solution.

Chemical admixture

A high range water reducer and retarding admixture was used to improve the workability of PCC mixtures. It complied with type G requirements according to ASTM C494 [34].

Mixtures

PCC mixture

Cement, aggregates, water and chemical admixture were mixed and cast with the proportions listed in Table 5 to produce an ordinary Portland cement concrete (PCC) of grade 30 MPa. PCC mix design was carried out according to absolute volume method as recommended in Egyptian Code of Practice [33] with several trails to achieve the required strength.

GPC mixture

Metakaolin (MK), aggregates, activator solution (AS) and water (W) were mixed and cast with the proportions listed in Table 5 to produce a GPC mix of grade 30 MPa according to GPC mix design guidelines [2, 16–18] that recommended the following data:

- MK per 1m^3 GPC = 320 kg.
- Ratios: W / Solids = 0.35

Na_2SiO_3 / NaOH = 2.5
AS /MK = 0.74

In this research, NaOH solution was prepared at 16 molars by adding 640 g of NaOH flakes to 500 ml of water and dissolving the flakes into water. The required amount of water was then added to make the solution reach 1000 ml and recorded (255 ml). Thus, the amount of water required to prepare 1000 ml of 16 molars NaOH solution was 755 ml to 640 g of NaOH flakes [35]. NaOH solution was left to cool at room temperature for 24 h to be handled because of the exothermic heat generated from NaOH dissolution process. After cooling, NaOH solution was then added to Na_2SiO_3 solution to produce the activator solution. Firstly, aggregates were mixed, and then, metakaolin was added to the mixed aggregates. Activator solution and extra water were then added [14–19].

Testing program

The testing program comprised compressive, flexural, and indirect tensile strengths tests. The program also included determining the static modulus of elasticity and Poisson's ratio. Fuel resistance and slab loading tests were also conducted. All GPC specimens were room temperature cured (Fig. 1), whereas all PCC specimens were water cured prior testing at various ages.

Fig. 1 Specimens of compression strength, flexure strength, modulus of elasticity and Poisson's ratio tests

Table 5 PCC and GPC (30 MPa) mix design per 1 m^3 of concrete

Type	MK	Cement	Sand	Agg. #20	Agg. #10	Water	Admix	Na_2SiO_3 Solution	NaOH Solution	Density (unit weight) (kg/m^3)
PCC components (kg)	–	400	730	540	540	180	5.8	–	–	2395.8
GPC components (kg)	320	–	530	620	620	20	–	170	68	2340

Compressive strength test

The test was conducted on PCC and GPC mixtures as per EN 12,390–3 [36]. The compressive strength test was performed on cubic specimens (100 × 100 × 100 mm) as shown in Fig. 2a at ages of 3, 7, 14 and 28 days.

Flexural strength test

Three-point load flexure test was performed as per ASTM C293 [37] on PCC and GPC specimens of dimensions 100 × 100 × 500 mm as shown in Fig. 2b at ages of 3,7 and 28 days. Flexural strength (modulus of rupture) is one of the main design criteria in all design methods and manuals [25–28]. Flexure strength test is also needed to evaluate the tensile strength [38].

Indirect tensile strength test

The test was performed as per ASTM C496 [39] on PCC and GPC cylindrical specimens of diameter 150 mm and 300 mm in height as shown in Fig. 2c at ages of 7 and 28 days.

Static modulus of elasticity and Poisson's ratio determination test

The test was performed as per ASTM C469 [40] on PCC and GPC cylindrical specimens of diameter of 150 mm and 300 mm in height at age of 28 days as shown in Fig. 3.

Fig. 3 Static modulus of elasticity and Poisson's ratio determination test

Fuel resistance test

As the resistance of pavement to fuel is one of the main catalysts for the use of concrete in paving, fuel resistance test was performed on PCC and GPC specimens as per EN 12,697-43 [41]. Test procedures included preparing three cylindrical specimens for each mixture (GPC and PCC) with a known mass as shown in Fig. 4a. The specimens were partially immersed in fuel bath (gasoline) for 72 h after the specimens' age reached 28 days as shown in Fig. 4b. The prepared specimens were removed from fuel bath, washed

(a) (b) (c)

Fig. 2 Characterization strength tests **a** compressive, **b** flexural and **c** splitting

(a) (b) (c)

Fig. 4 Fuel resistance test **a** GPC specimens, **b** fuel bath and **c** moving steel brush

Table 6 Fuel resistance evaluation as per EN 12,697-43:2014

Mass loss after fuel bath (*A*), (%)	Mass loss after fuel bath (*B*) and brushing, (%)	Fuel resistance category
$A<5\%$	$B<1\%$	Good
$A<5\%$	$1\%<B<5\%$	Moderate
$A>5\%$	$B>5\%$	Poor

with water and dried for 24 h at 25 °C in fully ventilated place and weighted to record any mass loss after fuel immersion. The sample surface that was immersed in fuel was later exposed to mechanical epicyclical moving steel brush for a period of 120 s as shown in Fig. 4c. The test was stopped every 30 s to inspect the brushed surface visually. The sample was then removed from the brushing device and weighted to determine the mass loss after brushing. Then, by calculating the average mass loss after fuel bath (*A*) and steel brushing (*B*), the fuel resistance was determined according to the three categories listed by EN 12,697-43 [41] as shown in Table 6.

Simulating subgrade soil

In order to simulate a subgrade soil with a specific modulus of subgrade reaction, a set of steel springs were used under a 20-mm recycled rubber layer (to ensure uniform stress distribution over all springs) as shown in Figs. 5a and b. A displacement control testing machine (Shimadzu 500 kN) was used to determine spring modulus of reaction (spring constant) in compression by recording the applied loads with the respective displacements. Spring modulus of reaction was 36 MPa/m.

(a) (b)

Fig. 5 Subgrade simulation **a** set of springs and **b** a 2-cm rubber layer

Slabs loading tests

The details of the test are demonstrated in Table 7 and Fig. 6. Three PCC slabs and three GPC slabs of dimensions (800 × 800 × 50 mm) were cast and tested under static load at interior, edge and corner positions. In this study, six concrete slabs were tested as each slab represents a load position for PCC and GPC mixtures as simulated in the previous studies [42, 43]. In these studies, the behavior of concrete pavement slabs was investigated with one slab for each load position and maintaining the surface dimension to thickness ratio greater than 15 which complies with the design assumptions as per design methods and manuals [25–28]. The load was monotonically applied at interior, edge and corner positions of the slabs using a hydraulic jack with linear variable displacement transducers (LVDTs) to measure the deflection under the loaded area. A steel frame was used to fix the concrete slabs with springs supports during the loading process. The steel frame contained three steel angles (50 × 50 × 5 mm) and one steel strip to fix the fourth side of the slab. Figure 7 shows the test setup at the three load cases and the four anchors that were used to fix the system completely.

Test results and discussion

Compressive strength

The compressive strength test of GPC and PCC mixtures was used as a measure to confirm that the mixtures had approximately the same compressive strength during the testing program. The behavior of GPC mixtures in gaining strength along curing age was observed. Table 8 shows PCC and GPC compressive strength test results. Metakaolin-based geopolymer concrete achieves approximately 80% of the required compressive strength at age 3 days and approximately 100% of the required compressive strength at age 7 days. For the same compressive strength, the required content of metakaolin was less than the required cement content.

Table 7 PCC and GPC slabs loading test

Slab material	Loading position	Slab code	Dimensions (mm)	Restraints
PCC	Interior	CI	800 × 800 × 50	Springs with k = 36 MPa/m
	Edge	CE		
	Corner	CC		
GPC	Interior	GI	800 × 800 × 50	Springs with k = 36 MPa/m
	Edge	GE		
	Corner	GC		

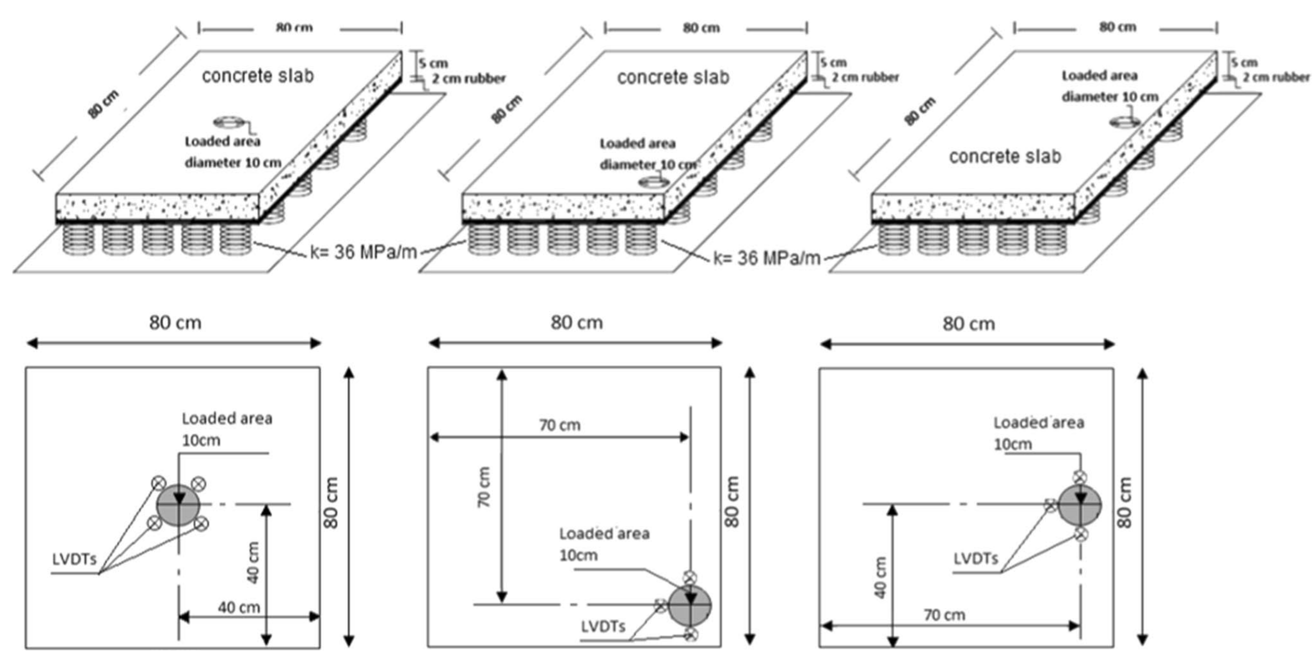

Fig. 6 PCC and GPC slabs loading cases (interior, corner and edge)

(a) (b) (c)

Fig. 7 Test setup for **a** interior, **b** edge and **c** corner loading cases

Table 8 Compressive, flexure and indirect tensile strength test results

Type	Ages	Compressive strength (MPa)	Flexural strength (MPa)	ITS (MPa)
PCC	3 days	14.0	4.7	–
	7 days	23.0	7.8	2.7
	14 days	26.8	–	–
	28 days	33.1	8.0	3.5
GPC	3 days	25.0	5.1	–
	7 days	30.3	7.6	2.8
	14 days	31.3		
	28 days	32.3	8.6	3.8

Based on the findings, GPC gained strength rapidly and this may be due to the rapid geopolymerization reaction and low water-to-solids ratio. Also, there was no need to use water reducer chemical additives as opposed in the case of PCC that resulted in some delay in both setting time and strength gain.

Flexural strength test

The flexural strengths of GPC and PCC mixtures were comparable as GPC achieved 8.6 MPa at age of 28 days with 7.5% increase when compared with PCC that achieved 8.0 MPa as shown in Table 8. Metakaolin-based geopolymer concrete (GPC) achieved approximately 98% of the 28-day flexural strength at age of 7 days, while PCC achieve approximately 88% of the 28-day flexural strength at age of 7 days. Based on the findings, GPC gained flexural strength rapidly as its compressive strength. This shows GPC is more efficient than PCC in concrete pavement regarding implementation rate, and as per concrete pavement design methods, the flexure performance of GPC indicates the feasibility to reduce the optimum thickness of concrete pavement slabs.

Indirect tensile strength test

Table 8 shows the slight increase in GPC indirect tensile strength (ITS) when compared with PCC, as GPC achieved 3.8 MPa at age of 28 days with 8.6% increase when compared with PCC that achieved 3.5 MPa. This, in turn, supports the aim of the study to present GPC as an alternative to PCC in concrete pavement slabs. This may be due to the cohesion and reactivity of metakaolin-based GPC with crushed stone aggregates.

Static modulus of elasticity and Poisson's ratio test results

As per ASTM C469 [40], PCC and GPC modulus of elasticity (E) and Poisson's ratio (μ) were determined using Eqs. (1) and (2) as shown in Table 9. The results clarify the convergence in E and μ properties for PCC and GPC.

Table 9 Modulus of elasticity (E) and Poisson's ratio test results

Parameters	PCC	GPC
Stress at longitudinal 50 micro strain ($S1$)	1.28 MPa	0.48 MPa
Stress at 40% of ultimate load ($S2$)	17.46 MPa	19.90 MPa
Longitudinal strain by stress $S2$ ($\varepsilon 2$)	0.000719	0.000833
Transverse strain by stress $S1$ ($\varepsilon t1$)	0.000010	0.000009
Transverse strain by stress $S2$ ($\varepsilon t2$)	0.000160	0.000190
modulus of elasticity for compression (E)	24,185 MPa	24,802 MPa
Poisson's ratio (μ)	0.224	0.231

Table 10 Fuel resistance test results

Parameters	PCC	GPC
Avg. initial mass (gram)	1376	1699
Avg. mass after fuel path (gram)	1371	1699
Avg. mass after brushing (gram)	1366	1694
Mass loss after fuel path, A (%)	0.00%	0.00%
Mass loss after brushing, B (%)	0.73%	0.29%
Fuel resistance category	A < 5%, B < 1% Good	A < 5%, B < 1% Good

$$E = \frac{S_2 - S_1}{\varepsilon_2 - 0.000050} \quad (1)$$

$$\mu = \frac{\varepsilon_{t2} - \varepsilon_{t1}}{\varepsilon_2 - 0.000050} \quad (2)$$

where S_1 is the stress at longitudinal 50 micro-strain, S_2 is the stress at 40% of ultimate load, ε_2 is the longitudinal strain by stress S_2, εt_1 is the transverse strain by stress S_1, and εt_2 is the transverse strain by stress S_2.

Based on the findings, metakaolin-based GPC provided more rigidity than PCC by 2.6% concerning rigid pavement slabs that result in a reduction in the transferred loads to the subgrade soil which is one of the main purposes to choose rigid pavement system rather than flexible pavement system.

Fuel resistance test results

As per EN 12,697-43 [41], PCC and GPC resistances to fuel were evaluated as shown in Table 10. The results indicated that GPC is more resistant to fuel than PCC and more resistant to surface abrasion by 60%. This makes GPC an appropriate choice as a paving material in fuel stations, garages, land ports and airports aprons.

Slab loading test results

Table 11 shows the test results of PCC and GPC slabs. Maximum applied loads (P exp.) and deflections (Δ exp.) in the three positions (interior—edge—corner) are listed. Figures 8, 9, 10 show the relations of interior, edge and corner applied loads versus vertical deflections under loaded area for PCC and GPC slabs. The maximum applied loads at the interior (GI), edge (GE) and corner (GC) load cases for GPC slabs were higher by 3.40%, 7.72% and 11.5%, respectively, when compared to the corresponding PCC slabs (CI), (CE) and (CC).

The total deflection at the interior (GI) and edge (GE) load cases for GPC slabs were lower by 15.26% and 18%, respectively, and higher by 12.74% for corner load case (GC) when compared to the corresponding PCC slabs (CI), (CE)

Table 11 Slabs loading test results

Slab material	Slab code	P exp. (kN)	Δ exp. (mm)
PCC	CI	735	13.1
	CE	653	25.5
	CC	668	31.4
GPC	GI	760	11.1
	GE	703	20.9
	GC	745	27.4

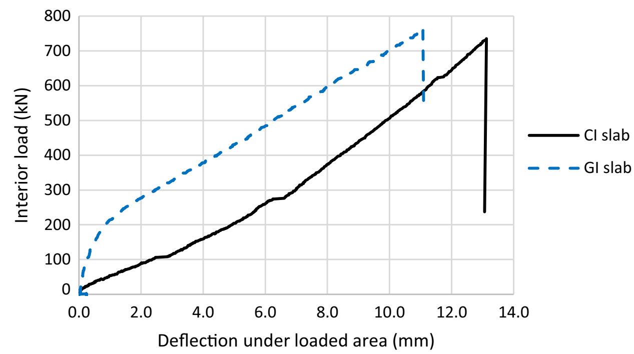

Fig. 8 Interior load versus deflection under loaded area of PCC and GPC slabs

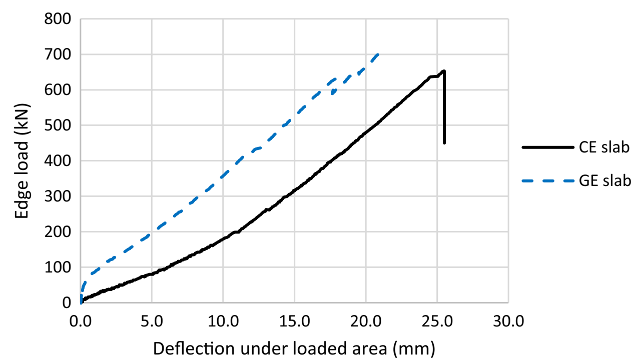

Fig. 9 Edge load versus deflection under loaded area of PCC and GPC slabs

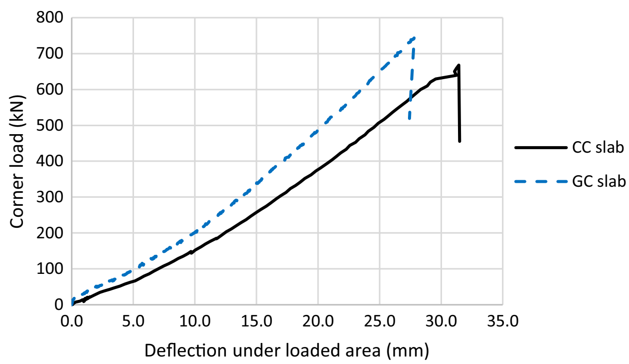

Fig. 10 Corner load versus deflection under loaded area of PCC and GPC slabs

and (CC). Based on the obtained results, GPC slabs present a comparable performance with PCC slabs due to mechanical loading tests. GPC gave higher load capacities for all load cases.

Conclusions

Compression, flexure and indirect tensile strength tests, fuel resistance test, modulus of elasticity and Poisson's ratio determination tests were performed on metakaolin-based geopolymer concrete (GPC) and Portland cement concrete (PCC). Six concrete slabs, three PCC slabs and three GPC slabs, were tested under monotonic static loads at three critical loading positions of the rigid pavement slabs: interior, edge and corner positions to investigate the possibility of using metakaolin-based geopolymer concrete (GPC) as an alternative paving material to PCC in rigid pavement sections. The tests results obtained showed that GPC (which is considered an eco-friendly concrete) is an adequate alternative to PCC as a rigid pavement slab material. Based on the results of the testing program, it was concluded that:

1. The required content of metakaolin in geopolymer concrete (GPC) mixture is less than the required content of cement in Portland cement concrete (PCC) mixture by approximately 20% to produce the same grade of concrete. This makes metakaolin-based GPC an adequate choice regarding economic and environmental considerations.
2. Metakaolin-based geopolymer concrete (GPC) accelerates rigid pavements implementation due to its early strength gain in ambient curing conditions, as GPC gains 100% of the required strength at the age of 7 days.
3. Modulus of elasticity and Poisson's ratio of metakaolin-based geopolymer concrete (GPC) are slightly more than those of Portland cement concrete (PCC), which indicate that GPC is more rigid than PCC.
4. Metakaolin-based geopolymer concrete (GPC) presents better performance regarding fuel resistance than Portland cement concrete (PCC), as the mass loss of GPC was lower than it was for PCC by 60.3%. Thus, GPC is an adequate choice for paving any site linked with petroleum leakage.
5. Metakaolin-based geopolymer concrete (GPC) slabs exhibited better performance where maximum load capacities at the three critical positions for GPC slabs were more than PCC slabs by 3.40% for interior loading case, 7.72% for edge loading case and 11.50% for corner loading case.
6. Metakaolin-based geopolymer concrete (GPC) slabs deflection was lower than Portland cement concrete (PCC) slabs by 18% at edge loading case, 15.26% at interior loading case and 12.74% at corner loading case. This may be because GPC is more rigid than PCC.
7. While the critical loading case for stress is edge loading case, GPC slabs present the highest improvement for load capacity and deflection (rigidity) in it.

Acknowledgements The authors are thankful to the team work of Housing and Building National Research Center, Egypt.

Funding None.

Declarations

Conflict of interest The authors declare that they have no conflict of interest.

References

1. Eisa MS, Basiouny ME, Fahmy EA (2021) Effect of metakaolin-based geopolymer concrete on the length of rigid pavement slabs. Innov Infrastruct Solut, 6(2) article no. 91. https://doi.org/10.1007/s41062-021-00465-5
2. Ferdous MW, Kayali O, Khennane A (2013) A detailed procedure of mix design for fly ash based geopolymer concrete. In: Proceedings of the Fourth Asia-Pacific Conference on FRP in Structures (APFIS 2013), Melbourne, Australia, 11–13
3. Alanazi H, Yang M, Zhang D, Gao ZJ (2016) Bond strength of PCC pavement repairs using metakaolin-based geopolymer mortar. Cem Concr Compos 65:75–82. https://doi.org/10.1016/j.cemconcomp.2015.10.009
4. Shekhawat P, Sharma G, Singh RM (2020) Potential application of heat cured eggshell powder and flyash-based geopolymer in pavement construction. Int J Geosynth Ground Eng, 6(2) article no. 28. https://doi.org/10.1007/s40891-020-00213-2
5. Xincheng P, Changhui Y, Fan L (1999) Studies on resistance of alkali activated slag concrete to acid attack. In: Proceedings of the 2nd international conference on alkaline cements and concretes, 717–722. Kyiev, Ukraine
6. Ariffin MAM, Bhutta MAR, Hussin M, Tahir MM, Aziah N (2013) Sulfuric acid resistance of blended ash geopolymer

concrete. Constr Build Mater 43:80–86. https://doi.org/10.1016/j.conbuildmat.2013.01.018
7. Bhutta MAR, Hussin WM, Azreen M, Tahir MM (2014) Sulphate resistance of geopolymer concrete prepared from blended waste fuel ash. J Mater Civ Eng 26(11):04014080. https://doi.org/10.1061/(ASCE)MT.1943-5533.0001030
8. Olubenga A, Onwualu AP, Boakye E (2021) Characterization and mechanical performance of metakaolin- based geopolymer for sustainable building applications. Constr Build Mater. https://doi.org/10.1016/j.conbuildmat.2020.121938
9. Rashad AM (2013) Metakaolin as cementitious material: History, scours, production and composition – A comprehensive overview. Constr Build Mater 41:303–318. https://doi.org/10.1016/J.CONBUILDMAT.2012.12.001
10. Davidovits J (1988) Geopolymer chemistry and properties. In: Proceedings of the 1st International Conference on Geopolymer, Compiègne, France, 1–3 June
11. Refaei DA, Abdelrahman MK, Ibrahim IA, Eldears F, Kandil AT (2017) Improvement the quality of Egyptian kaolin for industrial applications. Int J Adv Technol 8:174. https://doi.org/10.4172/0976-4860.1000174
12. Sinai Manganese Co. SMC website: https://www.smc-eg.com/MinKaolin.htm
13. Baioumy H, Albert Gilg H (2011) Pisolitic flint kaolin from Kalabsha, Egypt: a laterite-derived facies. Sediment Geol 236(1–2):141–152. https://doi.org/10.1016/j.sedgeo.2011.01.002
14. Castel A, Foster SJ, Ng T, Sanjayan JG, Gilbert RI (2016) Creep and drying shrinkage of a blended slag and low calcium fly ash geopolymer Concrete. Mater Struct 49(5):1619–1628. https://doi.org/10.1617/s11527-015-0599-1
15. Deb PS, Nath P, Sarker PK (2015) Drying shrinkage of slag blended fly ash geopolymer concrete cured at room temperature. In: Proceedings of the 5th International Conference of Euro Asia Civil Engineering Forum (EACEF-5), Surabaya, East Java, Indonesia, 15–18 September
16. Rangan BV (2008) Fly ash-based geopolymer concrete. Research report GC4, Faculty of Engineering, Curtin University of Technology, Perth, Australia. http://hdl.handle.net/20.500.11937/20680
17. Anuradha R, Sreevidya V, Venkatasubramani R, Rangan BV (2012) Modified guidelines for geopolymer concrete mix design using Indian standard. Asian J Civ Eng (Build Hous) 13(3):353–364. https://espace.curtin.edu.au/handle/20.500.11937/38772
18. Patankar SV, Ghugal YM, Jamkar SS (2015) Mix design of fly ash based geopolymer concrete. Adv Struct Eng New Delhi. https://doi.org/10.1007/978-81-322-2187-6_123
19. Wallah SE (2009) Drying shrinkage of heat-cured fly ash-based geopolymer concrete. Mod Appl Sci 3:14–21. https://doi.org/10.5539/mas.v3n12p14
20. Seneviratne C, Gunasekara C, Law DW et al (2020) Creep, shrinkage and permeation characteristics of geopolymer aggregate concrete: long-term performance. Archiv Civ Mech Eng. https://doi.org/10.1007/s43452-020-00119-w
21. Murmu AL, Patel A (2020) Studies on the properties of fly ash–rice husk ash-based geopolymer for use in black cotton soils. Int J Geosynth Ground Engineering, 6(3) article no. 38. https://doi.org/10.1007/s40891-020-00224-z
22. Lu D, Luo J, Xu Z (2015) Effect of metakaolin on the drying shrinkage behaviour of portland cement pastes. In: Scrivener K, Favier A (eds) Calcined clays for sustainable concrete, vol 10. RILEM Bookseries, Springer, Dordrecht
23. Güneyisi E, Gesoğlu M, Mermerdaş K (2008) Improving strength, drying shrinkage, and pore structure of concrete using metakaolin. Mater Struct 41:937–949. https://doi.org/10.1617/s11527-007-9296-z
24. Westergaard HM (1926) Analysis of stresses in concrete pavements due to variations of temperature. In: Proceedings of the Sixth Annual Meeting of the Highway Research Board Held, 6, 201–215, Washington D.C., 2–3 December
25. Portland Cement Association (1984) The design for concrete highway and street pavements. PCA, Skokie, Illinois
26. AASHTO (1993) Guide for design of pavement structures. American Association of State Highway and Transportation Officials; Washington DC, USA
27. Yoder EJ, Witczak MW (1975) Principles of pavement design, 2nd edn. Wiley, New York
28. FDOT (2009) Florida Department of Transportation. Rigid pavement design manual. Pavement Management Office, Document No. 625–010–006-e, Tallahassee, Florida
29. Suryawanshi NT, Thakare SB (2018) Self-curing assessment of Meta Kaolin based high strength concrete using super absorbent polymer. Int J Civ Eng Technol (IJCIET) 9(13):1082–1087
30. ASTM C618/C618M (2018) Standard Specification for Coal Fly Ash and Raw or Calcined Natural Pozzolan for Use in Concrete. ASTM International, West Conshohocken, PA
31. British Standards Institution BS EN 197–1 (2011) Cement: Composition, specifications and conformity criteria for common cements. London, UK
32. Egyptian Standard Specification (ESS) 4756-1 (2009) Composition, specifications and conformity criteria for common cements, Egyptian organization for standards and quality (EOS), Cairo, Egypt
33. Egyptian Code of Practice for Design and Construction of Reinforced Concrete Structures (ECP 203–2020). Ministry of Housing, Utilities and Urban Communities. Cairo, Egypt. 2020
34. ASTM C494/C494M (2019) Standard specification for chemical admixtures for concrete. ASTM International, West Conshohocken, PA
35. Rajamane NP, Jeyalakshmi R (2014) Quantities of sodium hydroxide solids and water to prepare sodium hydroxide solution of given molarity for Geopolymer Concrete mixes. Indian concrete institute journal, ICI update Aug.- Sep. 2014, 4:9
36. British Standards Institution BS EN 12390–3 (2014). Testing hardened concrete - Part 3: Compressive strength of test specimens. BSI, London, UK
37. ASTM C293/C293M (2016) Standard test method for Flexural Strength of Concrete (Using Simple Beam with Center-Point Loading). ASTM International, West Conshohocken, PA
38. Marathe S, Mithanthaya IR, Mithun BM, Shetty S, Akarsh PK (2020) Performance of slag-fly ash based alkali activated concrete for paver applications utilizing powdered waste glass as a binding ingredient. Int J Pavement Res Technol 14:196–203. https://doi.org/10.1007/s42947-020-0173-2
39. ASTM C496/C496M (2017) Standard test method for Splitting Tensile Strength of Cylindrical Concrete Specimens. ASTM International, West Conshohocken, PA
40. ASTM C469/C469M (2017) Standard test method for Static Modulus of Elasticity and Poisson's Ratio of Concrete in Compression. ASTM International, West Conshohocken, PA
41. British Standards Institution BS EN 12697–43 (2014). Bituminous mixtures: Test methods for hot mix asphalt. Resistance to fuel. BSI, London, UK
42. Hammons MI (1998) Advanced pavement design: Finite element modeling for rigid pavement joints, report II: Model development. DOT/FAA/AR-97/7; U.S. Army Engineer Waterways Experiment Station 3909 Halls Ferry Road, Vicksburg, MS 39180–6199; Office of Aviation Research, U.S. Department of Transportation, Federal Aviation Administration.
43. Al-Hedad ASA, Hadi MNS (2018) Effect of geogrid reinforcement on the flexural behaviour of concrete pavements". Road Mater Pavement Des 20(5):1005–1025. https://doi.org/10.1080/14680629.2018.1428217